*Transactions of the Materials Research Society of Japan* 29 [8] 3611-3613 (2004)

# Void Growth Simulations in Ni Crystal by using Molecular Dynamics and FEM

Tomoaki Tsuji
Chuo University, 1-13-27, Kasuga, Bunkyo-ku, Tokyo 112-8551, Japan
Fax: 81-3-3817-1820, e-mail: tsuji@mech.chuo-u.ac.jp

The void growth simulations in Ni crystal are proceeded by using Molecular Dynamics (MD) and FEM. The energy function of the hyper elastic material for FEM is determined in order to satisfy the mechanical properties, which are given by the potential function of the MD for Ni crystal. The same models are simulated by these different methods and the results are compared to each other.
Key words: void initiation, Ni, FEM, Molecular Dynamics, Simulation

## 1. INTRODUCTION

Formation of a void is a considerable feature for a number of engineering materials, because failure by coalescence of the voids is an important fracture mechanism in ductile solids. There are some theoretical solutions of the void formation for nonlinear elastic solid. On the other hand, it is important to study microscopic void formation, in order to consider the initiation of the void. We have been studying the void formation from a single seed by using Molecular Dynamics (MD) [1-3]. There are many studies about cracks by MD simulations. But, we think that the cracks cannot grow and exists as steady state in the atomistic level. If an atomic-order crack exists, it will immediately close by the inter-atomic power. Moreover the optimum configuration of the very small defect should be sphere by surface tension. By our void growth simulation, the atom-order void can exist in steady state by reducing the load.[2] But, the void growth phenomena should be dynamic. It is important to investigate void growth as dynamic phenomena.

Therefore, in this paper, the void growth simulations in Ni crystal are simulated by using MD and FEM. The energy function of the hyper elastic material for FEM is determined in order to satisfy the mechanical properties, which are given by the potential function of the MD for Ni crystal. The same models are simulated by these three different methods and the results are compared to each other.

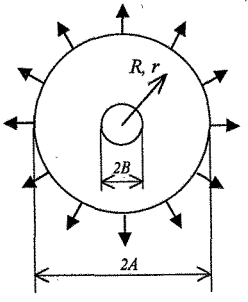


Fig.1 The configuration of the model with a hole. The values on the reference coordinate and on the deformed coordinate are denoted by capital letters and small letters, respectively.

## 2.GOVERNING EQUATIONS OF HYPER ELASTICS

The infinite cylinder subjected to equivalent stretch was studied by Biwa[4], by using the following energy function $w$.

$$w=\frac{\mu}{k}(\lambda_1^{-k}+\lambda_2^{-k}+\lambda_3^{-k})+\mu(\lambda_1\lambda_2\lambda_3-1) \qquad (1)$$

where $\lambda_i$ ($i$ = 1, 2, 3) denotes the principal stretch. In this study, the dynamic simulations are proceeded by using this energy function. If the deformation is uniform along the axis $X$, the kinetic equation is given as follows[5].

$$\frac{dt_1^{(1)}}{dX}=\rho\frac{\partial^2 x}{\partial t^2}, \qquad (2)$$

where, $X$, $x$, $t_1^{(1)}$, and $\rho$ denote the reference coordinate, the deformed coordinate, the Cauchy stress tensor, and density, respectively. $t_1^{(1)}$ is given by the energy function as

$$t_1^{(1)}=\frac{\partial w}{\partial \lambda_1}=\mu(\lambda-\lambda^{-k-1}). \qquad (3)$$

In the uniform stretch along $X$ direction, $\lambda_2$ and $\lambda_3$ equal 1, and $\lambda_1$ is uniform along $Y$ and $Z$ direction. In consideration with Eqs. (1) and (3), Eq. (2) can be written as follows.

$$\frac{\partial^2 x}{\partial t^2}=\frac{\mu(k+1)}{\rho}\lambda_1^{-(k+2)}\frac{\partial^2 x}{\partial X^2}. \qquad (4)$$

In the small deformation case, the sound speed $c$, the longitudinal modulus $E$, shear modulus $G$ and poison's ratio $\nu$ are obtained as follows.

$$c=\sqrt{\frac{\mu(k+1)}{\rho}\lambda_1^{-(k+2)}}\cong\sqrt{\frac{\mu(k+1)}{\rho}},$$

$$E=\sqrt{\frac{k+3}{k+2}}\mu k,\quad G=\frac{\mu k}{2},\quad \nu=\frac{1}{k+2}. \qquad (5)$$

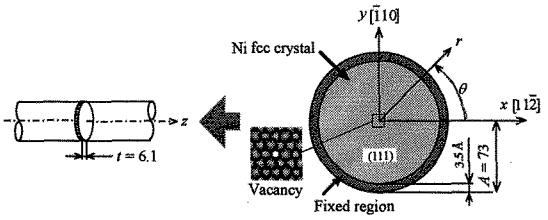


Fig.2 The simulation model.

## 3. SIMULATION BY MD AND FEM

### 3.1 Molecular Dynamics Simulations

Consideration will be focused on the atom-order void in the defective infinitely long cylinder under external tensile load. The basic cell has a shape of a thin circular plate shown in Fig. 2. The simulation model is constructed with fcc crystal of 9327 Ni atoms on (111) plane. The outer surface of the cylinder is fixed in order to deform the cylinder along the radial direction. A vacancy is given to the center of the model as a microscopic defect. The periodic repetition of the basic cell generates a line of vacancies, which can be viewed as an atom-scale void. This void will play the role of a seed to a large void.

In the MD simulations presented here, Newton's equations of motion of atoms are solved by using Verlet algorithm with the time step 1.0[fs]. Embedded Atom Method (EAM) by Foiles, Baskes and Daw [6] is used as the inter-atomic potential. The tensile stretch $\lambda$ is increased from 1.0 to 1.2 by the stretch velocity 1.0 [1/ns]. Temperature control in the relaxation is performed at every 200 time steps (=20[fs]) by scaling the velocity of the atoms. While the external load is being applied, the temperature control is not carried out. Figure 3 shows the snapshots of the void in the cylinder subjected to the equi-triaxial stretch. The stretch velocity for expansion process is 1.0 [1/ns]. The void is nucleated by the breaking of the inter-atomic bonds near the vacancy. In this simulation, the critical stretch $\lambda_C$ at which the void begins to develop is 1.069. The restricted region near the void surface spreads toward the outer surface with the expansion of the void. This region finally covers all over the region of the cylinder, and the initial perfect crystal disappears. The developing void keeps in an axisymmetric cylindrical hole.

### 3.2 FEM Simulations (Static)

By using the energy function $w$ given by Eq.(1), FEM simulations with an initial void, which has radius $B$, are proceeded. Figure 4 shows the snapshots of the void growth with the equi-triaxial stretch. The void begins to grow by $\lambda = 1.1$ in Fig.4. The relationships between the non-dimensional void radius $r(B)/A$ and the stretch $\lambda$ for the equi-triaxial and the plain strain stretch are shown in Fig.5. In the figure, the values by the MD simulations and the theoretical solutions are shown by solid circles and dotted lines, respectively. The FEM values are converged to the theoretical solution with decreasing the initial void radius $B$. By the theory for the non-linear elastic material, the void radius increases continuously with the increment of the stretch $\lambda$. On the other hand, by the MD simulation, there is a discontinuous expansion of the void at the critical stretch.

### 3.3 FEM Simulations (Dynamic)

The non-linear elastic simulations are proceeded by using FEM. The coefficients $\mu$ and $\kappa$ in Eq. (1) are obtained as 131GPa and 1.226, respectively, in order to agree with the longitudinal elastic modulus 210GPa and poison's ratio 0.31. The density is set as $\rho = 8910\text{kg/m}^3$. The sound speed can be given as $c = 5.716\times10^3$[m/s] by Eq.(5). The simulations proceed as follows.

1) Apply the homogeneous deformation by stretching uniformly along $R$ direction as follows:

$$r = \lambda R. \tag{6}$$

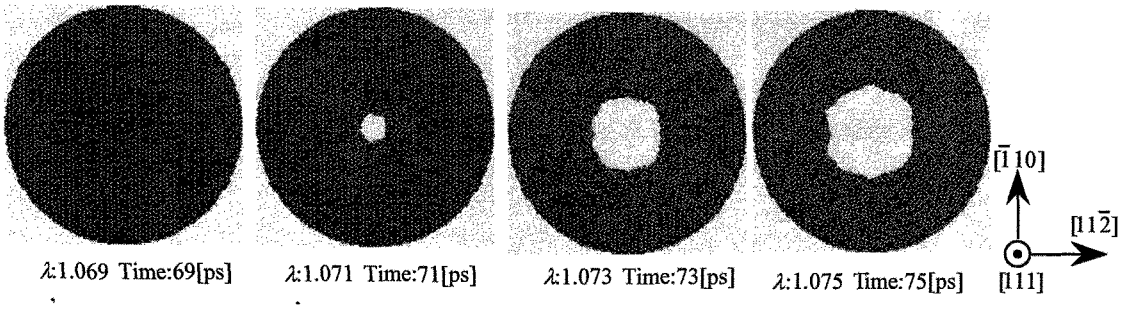


Fig.3 Snapshots of the void growth.

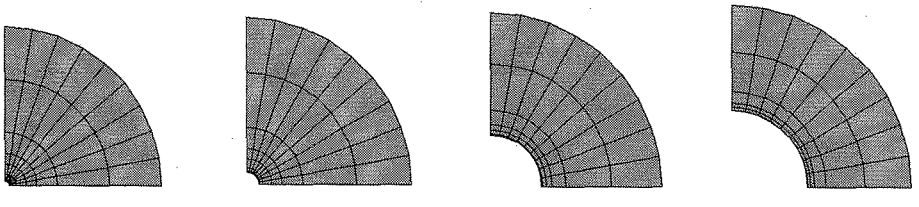


Fig.4 The void growth for the equi-triaxial stretch by the FEM simulation. ($B/A = 0.0166$, $\lambda_x = \lambda_y = \lambda_z = \lambda$)

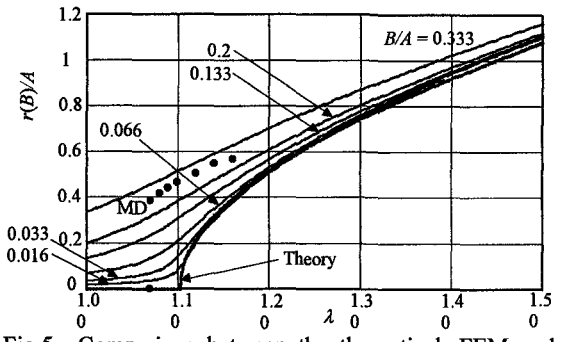


Fig.5 Comparison between the theoretical, FEM and MD simulation for the equi-triaxial deformation. The relationships between the non-dimensional radius of the void and the stretch are shown.
($\lambda_x = \lambda_y = \lambda_z = \lambda$)

2) Fix the outer surface and release the inner surface at time $t = 0$.
3) Proceed the dynamic, large deformation and nonlinear simulation.

Figure 6 shows the time dependence of the inner radius $a$ with the hole radius $B/A$ = 0.05 and the initial stretches $\lambda$ = 1.1 to 1.3. The inner radius begins to increase as soon as the constrain of the inner surface becomes free. And the inner radius begin to oscillate, because waves reach the outer surface and back to the inner surface. When the initial stretch $\lambda$ increases as $\lambda$ = 1.1 to 1.3, the maximum radius of the hole becomes bigger and the growth speed of the hole becomes rapid. The position of the head of stress wave, which starts at $t$ = 0 and has the speed given by Eq.(5), from the inner surface is shown in Fig.6 by the dotted line. The speed of the hole growth with $\lambda$ = 1.3 is about half of the stress wave speed.

Figure 7 shows the maximum radius of the hole with respect to the initial stretch $\lambda$. The values obtained by the static simulation are shown by the solid line. In this figure, the difference between the dynamic values and the static values becomes large in the neighborhood with $\lambda$ = 1.2.

## 4. CONCLUSIONS

A little difference of the initial defects makes huge difference of the void growth in the hole growth simulations with several initial defects.[7] It is investigated by the present study that the radius of the initial void is related to the maximum radius of the void. Thus, in the actual void growth, many initial defects influence each other dynamically. It must be the very complex phenomena. Especially, in the atomistic level, it happens complex void growth and coalescence in the very small time scale.

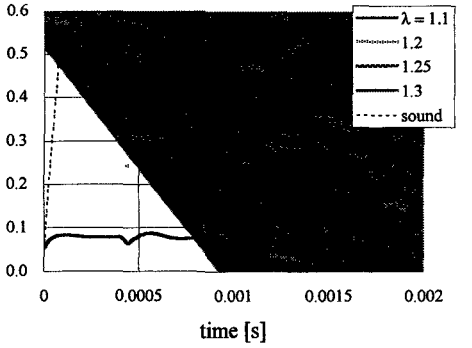


(a) time = 0 – 0.002 [s]

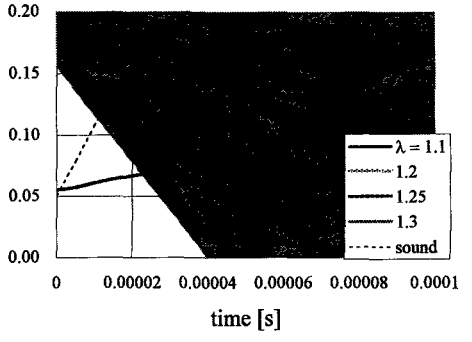


(b) time = 0 – 0.0001 [s]

Fig.6 Time dependence of the radius of the void. The stress wave is denoted by dotted line. ($B/A$ = 0.05)

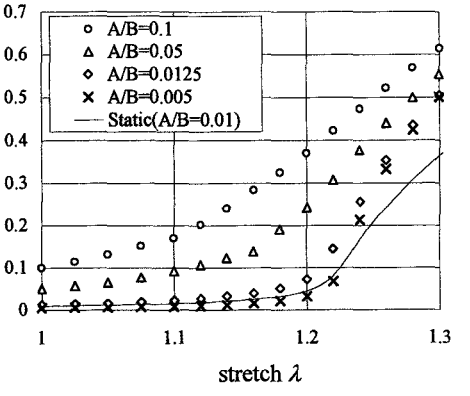


Fig.7 The relationship between the stretch and the maximum radius of the voids with various values of the initial hole radius. The results by the static simulation with $B/A$ = 0.01 is shown by the dotted line.

[1] M. Makino, T. Tsuji and N. Noda, Proc. JSSUME'98 (ISBN 89-7581-073-9 93550), 53-54, (1998).
[2] M. Makino, T. Tsuji and N. Noda, Computational Mechanics **26**, 281-287, (2000).
[3] T. Tsuji, M. Makino and N. Noda, Advances in Comput. Eng. & Sciences **II**, 1168-1173, (2000).
[4] S. Biwa, Int. J. Non-Linear Mech. **30-6**, 899-914, (1995).
[5] R. W. Ogden, "Non-Linear Elastic Deformations", Dover (1997), pp.231.
[6] S.M. Foiles, M.I. Baskes and M.S. Daw, Phys. Rev. B **33**, 7983, (1986)
[7] T. Tsuji and N. Noda, 6th U.S. National Congress on Computational Mechanics, 172, (2001).

(Received October 24, 2003; Accepted September 21, 2004)